Flight Test Results for An Improved Line of Sight Guidance Law for UAVs

Mariano Lizarraga[1], Renwick Curry[2] and Gabriel Hugh Elkaim[3]

***Abstract*— This paper presents flight test results of a new line-of-sight guidance law used onboard the University of California Santa Cruz' UAV. The architecture, as implemented onboard the UAV's autopilot, is presented and its key advantages are discussed. To show the guidance law's versatility, the paper presents its usage in three common scenarios that arise when working with small UAVs: (1) Navigation of straight-line waypoint arrays, (2) circular orbiting above a given point of interest, and (3) return to base, either as a safety measure or as an end-of-mission order. Flight test results for these three scenarios are presented and discussed.**

I. Introduction

Unmanned Aerial Vehicle (UAV) usage has exploded in the recent years. Fueled by multiple factors, but mainly due to the commoditization of the onboard components, UAVs are becoming ubiquitous. Today UAVs are used, besides the typical law enforcement and military applications, for ship-board oil pollution monitoring and detection[1], agricultural multi-spectral imaging[2], soil erosion monitoring[3], and even as off-the-shelf high-end toys[4]. This wide variety of applications show the UAV's potential as a support tool and reflect the noticeable decrease in size and price-tag they've had in the last decade.

Regardless of the end use given to the UAV, one key component to make it autonomous is the *Guidance* system. This system takes into account the UAV's state and, based on the currently defined mission, generates the state trajectory the UAV should follow in accomplishing its mission. Thus, it is this system that enables the ground operator to issue high-level commands, such as "orbit this point" or "follow this path".

Guiding a vehicle along a desired trajectory is a problem that has been widely studied. In the most general sense, this type of problems can be classified in two categories[5]:

- **Trajectory tracking**: Where the vehicle in motion is controlled to track a time-parameterized trajectory.
- **Path following**: Where the vehicle in motion is controlled to track a trajectory with no temporal constraints.

In the context of UAVs, trajectory tracking is employed when time is a critical factor in the end application, such as in formation fight[6][7], rendezvous, or cooperative control of multiple UAVs[8]. The guidance law discussed in this paper, falls in the second category: path following. The overarching idea for this law was developed for ground robots[9] and later extended for UAVs by Park *et al.*[10][11]. In this guidance law the lateral acceleration is commanded to follow the instantaneous circular path from the vehicle to the reference path a fixed distance away. The end result is the same as pursuit tracking originally used for air-to-air missiles where the only difference is that the "target" is always at a fixed range and thus never reached. Although Ref. [11] proved Lyapunov stability for tracking circular paths and straight lines with this method, it assumed that the lateral acceleration response to such commands is instantaneous, which is hardly the case. The real dynamics and response time of the bank angle to commanded acceleration was shown to cause instability[12].

The flight test results presented in this paper make use of the guidance law introduced by the authors in Ref [12]. The architecture discussed is that implemented on the SLUGS autopilot[13][14][15] used with UC Santa Cruz' UAV (a Multiplex Mentor).

The rest of this paper is structured as follows: Sec. II presents a brief overview of the new nonlinear guidance law as presented in Ref. [12]. Sec. III describes the *Guidance* system architecture as implemented in the research UAV used at the University of California Santa Cruz and discusses how the same guidance law is used to accomplish three common objectives of UAV guidance: waypoint array line tracking, circular orbiting about a point of interest, and homing on a point of interest. To show the versatility of the system's architecture, flight test results are presented and discussed in Sec. IV. Sec. V concludes the paper.

II. L_2^+ Guidance Law

The guidance law discussed in this section follows from that first presented by Amidi[9] for ground vehicles, then applied to UAVs by Park, Deyst, and How[10][11], and later extended by Curry[12]. Conceptually, this guidance law steers the velocity vector toward the line of sight, and thus is a form of pursuit guidance similar to the ones originally used in air-to-air missiles. For the remainder of the paper, we refer to this guidance law as L_2^+ guidance as presented in Ref. [12].

Based on the geometry shown in Fig. 1, let V_g be the UAV's horizontal velocity vector with respect to the ground and C be a circular arc of radius R that lies tangent to the velocity vector and passing through the UAV position.

Let L_1 be a constant lookahead distance from the UAV position to the path in the desired direction of travel. The circular arc C passes through the intersection of this distance with the desired path and is fully described by its two end

Department of Computer Engineering, University of California Santa Cruz, Santa Cruz, CA 95064, USA
[1]malife, [2]rcurry, [3]elkaim at soe.ucsc.edu

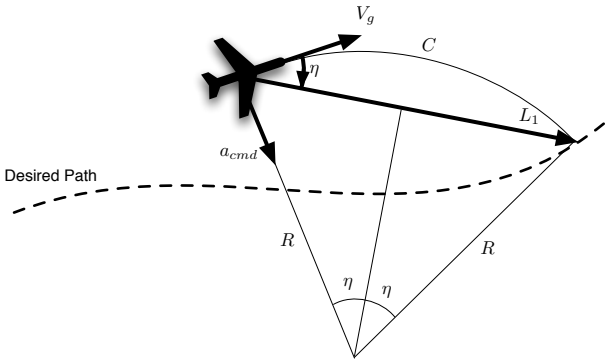

Fig. 1: Line of sight geometry. After Fig. 1 in Ref. [10]

points and radius R. This L_1 vector is divided into two equal segments by the line that bisects the chord defined by the circular arc C. Then from elementary trigonometry:

$$\frac{|L_1|}{2} = R \sin\eta. \tag{1}$$

Additionally, from elementary kinematics it is known that the centripetal acceleration, a_c, required to follow the circular arc C is given by:

$$a_c = \frac{|V_g|^2}{R}. \tag{2}$$

Therefore to follow the arc C the UAV must command a lateral acceleration of a_c. Solving Eq. 1 for R and substituting it into Eq. 2 produces the following guidance law for commanded acceleration:

$$a_{cmd} = 2\frac{|V_g|^2}{|L_1|}\sin\eta. \tag{3}$$

A small angle analysis of the guidance law in Eq. 3 presented in Ref. [11] shows that the following transfer function describes the response of the system:

$$G(s) = \frac{\omega_n^2}{s^2 + \zeta\omega_n s + \omega_n^2}, \tag{4}$$

where

$$\begin{aligned} \zeta &= 0.707, \\ \omega_n &= \sqrt{2}\frac{|V_g|}{|L_1|}. \end{aligned} \tag{5}$$

Note that the pole location depends only on the system characteristic time $T \equiv |V_g|/|L_1|$ and thus moves as V_g changes. To alleviate this, the look ahead distance, L_1, is changed so that the pole location is independent of groundspeed: this is done by modifying Eq. 3 to calculate the look ahead distance as a function of groundspeed:

$$|L_2| = T^*|V_g| \tag{6}$$

where T^* is a constant. The natural frequency of the linearized response is $\sqrt{2}/T^*$, which is independent of ground speed. Substituting Eq. 6 into Eq. 3 provides the L_2^+ guidance law:

$$a_{cmd} = 2\frac{|V_g|}{T^*}\sin\eta. \tag{7}$$

It is clear that the only requirements for the implementation of this control law are to selected the constant T^* and to determine $\sin\eta$.

1) Choosing T^*: Ref. [12] performed a stability analysis of the pursuit guidance laws that included the dynamics of the UAV roll response dynamics. The roll response was modeled as a first order lag to commanded bank angle with time constant τ_{roll}. This showed the destabilizing effects of the roll response when the characteristic time $T = |V_g|/|L_1|$ of the L_1 guidance is close to the roll time constant τ. In fact, it was shown that the system is marginally stable when $T = \tau$, so T^* should be chose 3 or 4 time larger than τ for good transient response.

2) Calculating $\sin\eta$: The angle η is sometimes called the line of sight angle. T^* is analogous to feedback gain, with larger values corresponding to smaller gains.

The quantity $\sin\eta$ is found from the vector cross product of V_g and L_2.

$$\sin\eta = \frac{V_g \times L_2}{|V_g||L_2|}. \tag{8}$$

For the UAV to actually track the desired trajectory, the lateral acceleration command, a_{cmd} computed in Eq. 7 must be converted to an appropriate bank angle command ϕ_{cmd} using the steady-state turn equation for an aircraft:

$$\phi_{cmd} = \tan^{-1}\left(\frac{a_{cmd}}{g}\right). \tag{9}$$

However, it is necessary to limit the bank angle to some specified level, ϕ_{max}, to avoid extreme attitudes when η is close to 90°. Limiting ϕ implies a limit on η. This limit on η is also useful so that a maximum acceleration (bank angle) is achieved when $\eta \geq 90^\circ$. In Ref. [12] this limit on η is:

$$\eta_{max} = sin^{-1}\left(\frac{T^* g \tan\phi_{max}}{2V_g}\right) \tag{10}$$

from which the bank angle commands become:

$$\phi_{cmd} = \begin{cases} -\phi_{max} & \eta \leq -\eta_{max} \\ tan^{-1}\left(2\frac{|V_g|}{gT^*}\sin\eta\right) & |\eta| < \eta_{max} \\ \phi_{max} & \eta \geq \eta_{max}. \end{cases} \tag{11}$$

The reader is further referred to Ref. [12] for a complete analysis of the L_2^+ guidance law as well as the extensions to account for the case when the UAV is farther than $|L_2|$ from the desired path.

III. Guidance Law Architecture

The L_2^+ guidance law, briefly discussed in the previous section and presented in Ref. [12], is independent of the desired trajectory. One only needs to define the vector L_2 to compute $\sin\eta$ and from that generate lateral acceleration commands. The L_2 vector is always defined if there is an "aim point" defined, and the definition of an aim point is the central tenet of the L_2^+ guidance law. This fact lends itself to have multiple independent ways to compute the aim point (L_2 vector) based on the the mission under which the UAV is operating. Fig. 2 shows the architecture implemented in

SLUGS for three different modes: Return to base, waypoint tracking and point of interest (POI) orbiting. Each of these modes is enabled based on the current mission mode. The enabled block's L_2 vector is then passed to the navigation law which generates the acceleration command to the inner-loop autopilot.

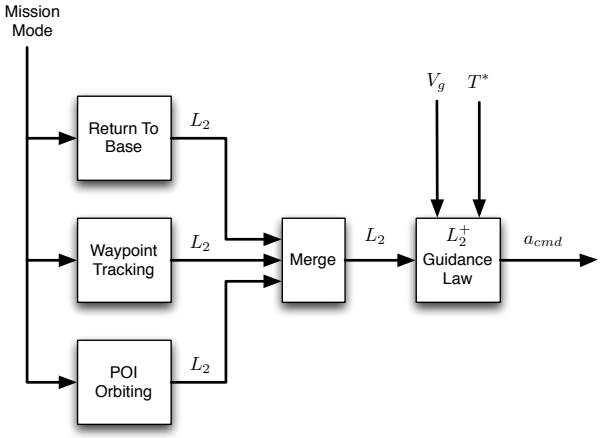

Fig. 2: Guidance law architecture implementation in SLUGS

The following subsections give a brief description of each mode.

A. Return to Base (RTB)

The RTB mode is implemented with the homing mode of L_2^+ to have the UAV return to some specified point on the ground. This becomes the aim point. In this mode there is no defined path, but the aim point is defined, generally the Ground Control Station. The basic guidance law of Equation 7 is still used. When the UAV reaches the base (aim point) it continues to try to fly over the base and begins an immediate maximum bank turn to do so. This continues with multiple passes over the base in a pattern determined on each pass by the wind and approach geometry.

B. Waypoint Tracking

When the UAV is "near" to the line (path) between waypoints, the aim point is defined by the intersection of the path with a circle of radius $|L_2|$. The $|L_2|$ vector connects the UAV with this intersection point.

When the UAV is "far" from the path, the aim point is defined by three different rules: (1) the intercept angle of the L_2 vector is limited to a specified value; (2) a down-path distance is defined for cases when the lateral distance from the path is large; and (3) no aim point is allowed to go beyond the active waypoint.

C. POI Orbiting

The objective in POI orbiting is to have the ground path of the UAV describe a circle of specified radius around the point of interest. The following logic was used to determine the aim point for the L_2 vector:

- If the UAV *is* within $|L_2|$ of the circular ground track, then the aim point is the intersection of the circular ground track and a circle of radius $|L_2|$ centered at the UAV.
- If the UAV is *not* within $|L_2|$ of the circular ground track,
  - If the UAV is inside the circular ground track, the homing mode is initiated with the aim point as the north-most point of the circular ground track. The UAV flies toward it until the it is within $|L_2|$ of the circular ground track
  - If the UAV is outside the circular ground track, the homing mode is initiated with the aim point as the center of the circle until the UAV is within $|L_2|$ of the circular ground track

IV. Flight Test Results

The fundamental advantage of the SLUGS autopilot is its tight integration with MATLAB/Simulink. The overall "software simulation→ hardware-in-the-loop simulation→ flight tests" process is as follows:

- Designs are first developed in a Simulink model and tested in software simulation, where the guidance, navigation, and control (GNC) algorithms interact with a full 6DOF flight model of the aircraft.
- The Simulink model is then compiled and downloaded to the SLUGS autopilot and installed in the hardware-in-the-loop Simulator for real-time testing of hardware performance
- The final step are flight tests, where the autopilot now uses its onboard sensors data (instead of the simulated one from the HIL simulator) to control the aircraft.

This section presents some of the many results obtained during this last step: flight tests. The SLUGS autopilot was installed in an off-the-shelf hobby electric model aircraft, the Multiplex Mentor. It is a very benign aircraft with an endurance of approximately 15 minutes on its battery.

The first flight tests were performed to validate the three modes of autopilot operation. These tests occurred during the month of July and although the flight results presented in this section are from different days of flight, the weather conditions were very similar.

A. Waypoint Tracking Results

These tests were designed to show two particular things **(i)** Capture of the initial waypoint array even if the UAV is far from it, and **(ii)** Guidance law performance during multiple passes in the waypoint array.

Fig. 3 shows a green square where the waypoint tracking mode is enabled. From there the UAV flies around and enters the waypoint array and successfully starts traversing it.

Fig. 4 shows an instance where a different waypoint array is traversed by the UAV and exhibits very similar behavior between passes.

These initial tests of SLUGS' waypoint tracking capabilities showed that its performance matched expectations, and tests proceeded to the next phase.

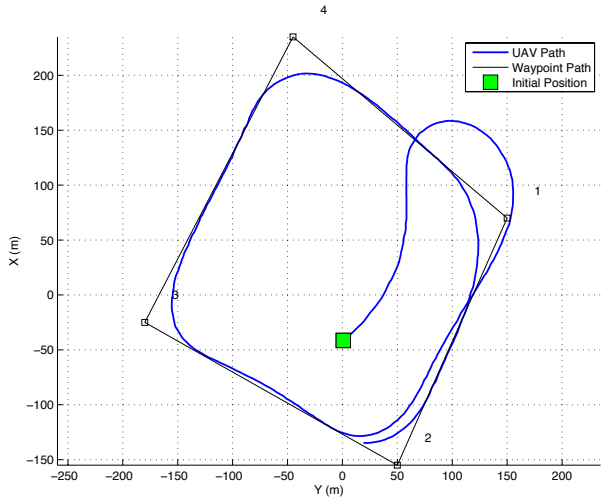

Fig. 3: Waypoint Tracking. Intial Capture of the WP Track.

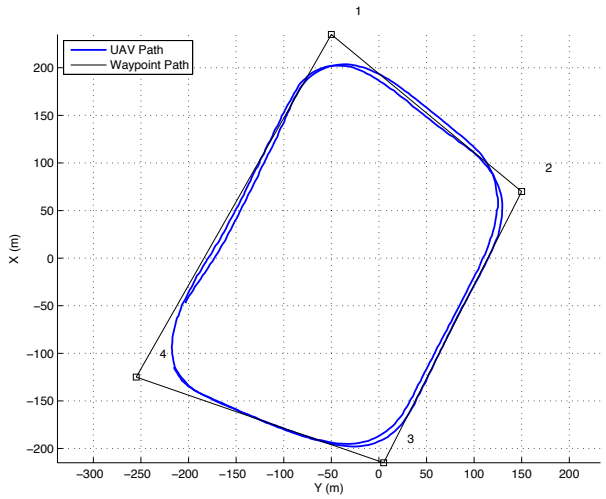

Fig. 4: Waypoint Tracking. Performance under multiple passes.

B. POI Orbiting Results

The second series of tests were aimed at showing the POI orbiting and how it performed under different wind conditions. The results in Fig. 5 show the POI orbiting mode being enabled when the UAV is inside the circle. As described in Sec. III, the UAV started flying toward the north-most point in the circle track. At the moment the L_2 vector intersected the desired track, the UAV started tracking the circular track. Performance is consistent through multiple traversals of the desired path.

C. Return To Base Results

The final mode tested was the Return To Base mode which was considered a critical safety net in case of loss of communication (i.e. losing the communications RF link between the ground control station and the UAV). For this test, shown in Fig. 6 the safety pilot had the UAV take off manually, and control was transferred to the autopilot at a remote location (green square), near to a POI. While in POI orbiting mode, the UAV was ordered to return to base. Once the UAV reached the ground station location (yellow triangle) the airplane kept flying over it until the safety pilot took control and landed it.

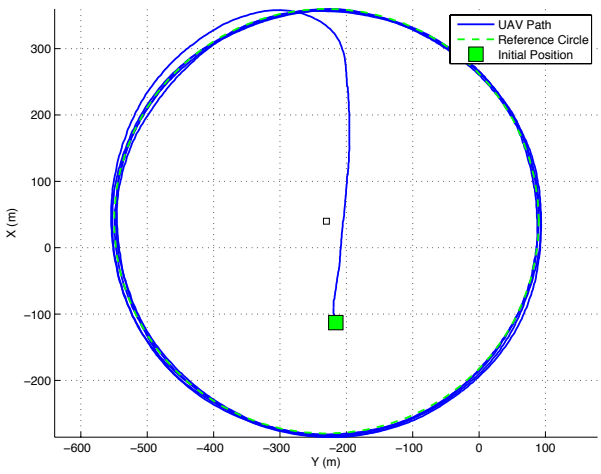

Fig. 5: POI Orbiting

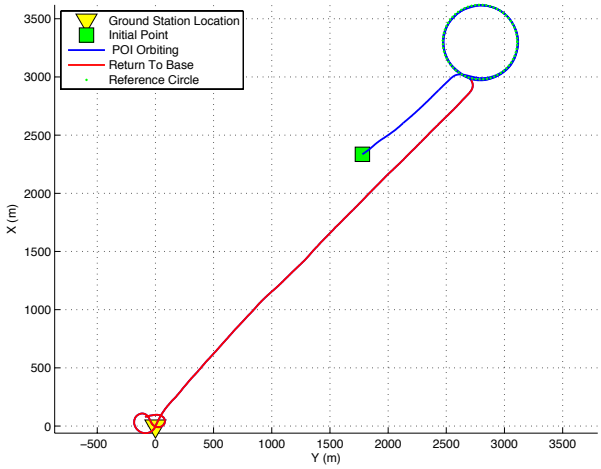

Fig. 6: Return To Base

D. Mixed Operations Results

The last set of experiments tested several modes simultaneously. Fig. 7 shows a sample of this set of experiments.

Here, the pilot flew the takeoff phase in manual mode (green) and then transferred the control to SLUGS in Waypoint Tracking mode (red). In this mode the UAV traversed 6 waypoints before being commanded to circle two different POIs before reaching waypoint 7. The first POI is only flown for approximately half a turn before being commanded to the next POI where it orbited for several turns.

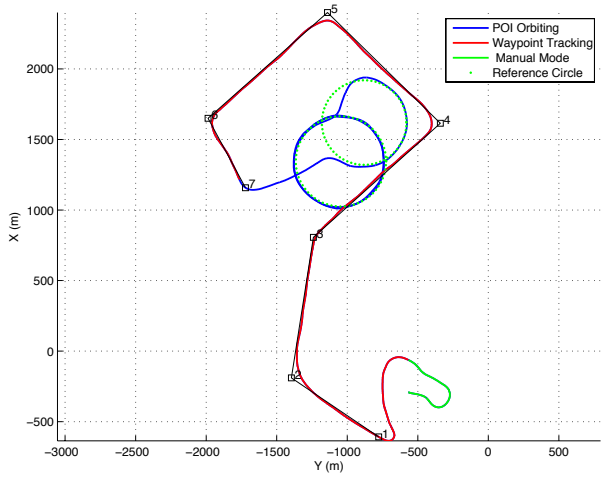

Fig. 7: Waypoint Tracking and POI Orbiting in the same mission.

E. Follow a Mobile Ground Station

In the RTB mode, there is a well defined aim point but no specified path. There is nothing limiting the UAV to "return" to a stationary point, and, conceptually, the UAV can follow a moving vehicle in this mode if its position is known. To test this hypothesis, the safety pilot and ground station were placed onboard a pickup truck with the safety pilot monitoring the UAV. Fig. 8 shows four snapshots of the same experiment.

The UAV first orbited the stationary truck, and then the truck moved along the street, shown in the upper left snapshot with the UAV following it. In the upper right and lower left snapshots the truck needed to slow down for the turns in the road, and the UAV started "S" turns to slow down and stay with the truck. In the lower right snapshot one can see the truck has reached its destination and the UAV orbits on top of it.

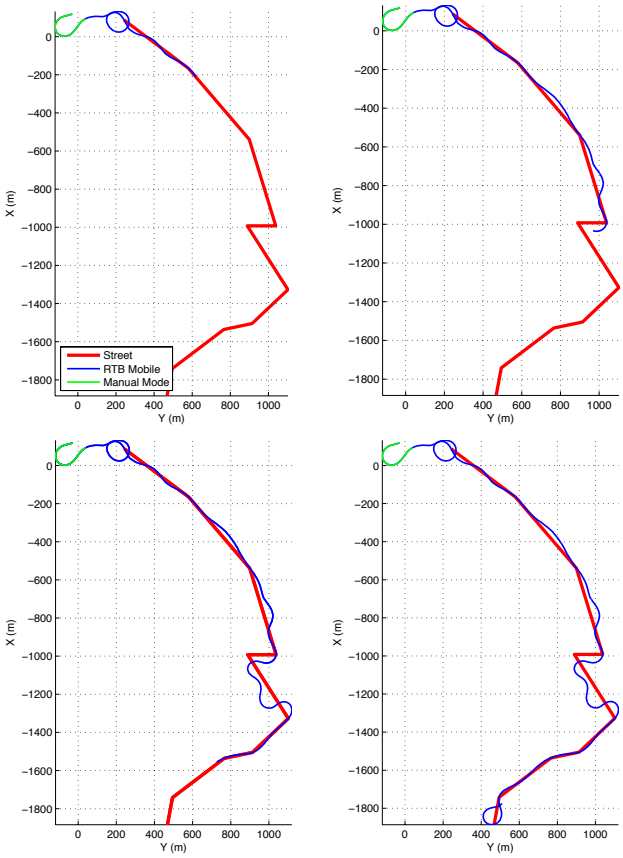

Fig. 8: Following a Mobile Ground Station

V. Conclusions

This paper has presented multiple flight test results for the L_2^+ line of sight guidance law and the architecture as implemented onboard the SLUGS autopilot. These flight tests validate what was presented in Ref. [12] with software simulation results only and show the guidance law and the architecture to be a versatile and yet easy to implement.

References

[1] F. Muttin, "Umbilical deployment modeling for tethered uav detecting oil pollution from ship," *Applied Ocean Research*, vol. 33, no. 4, pp. 332 – 343, 2011.

[2] T. A. Martin De Biasio and R. Leitner, "UAV based Multi-spectral Imaging System for Environmental Monitoring," *tm - Technisches Messen*, vol. 78, no. 11, pp. 503–507, November 2011.

[3] S. d'Oleire Oltmanns and I. Marzolff, "UAV derived data for the monitoring of gully erosion in the Souss Basin, Morocco," in *European Geosciences Union General Assembly Conference*, vol. 14, 2012, p. 911.

[4] P. Bristeau, F. Callou, D. Vissière, N. Petit, *et al.*, "The navigation and control technology inside the ar. drone micro uav," in *18th IFAC World Congress, Milano, Italy*, 2011, pp. 1477–1484.

[5] D. Soeanto, L. Lapierre, and A. Pascoal, "Adaptive, non-singular path-following, control dynamic of wheeled robots," in *International Conference on Advanced Robotics*, June 2003, pp. 1387–1392.

[6] C. B. Low, "A trajectory tracking control design for fixed-wing unmanned aerial vehicles," in *IEEE International Conference on Control Applications*, Japan, September 2010, pp. 2118–2123.

[7] H. Min, F. Sun, and F. Niu, "Decentralized uav formation tracking flight control using gyroscopic force," in *International Conference on Computational Intelligence for Measurement Systems and Applications*, 2009.

[8] I. Kaminer, O. Yakimenko, V. Dobrokhodov, A. Pascoal, N. Hovakimyan, C. Cao, A. Young, and V. Patel, "Coordinated path following for time-critical missions of multiple UAVs via $\mathcal{L}_1$ adaptive output feedback controllers," *AIAA Guidance, Navigation and Control Conference and Exhibit*, August 2007.

[9] O. Amidi and C. Thorpe, "Integrated mobile robot control," *Proc. SPIE*, vol. 1388, no. 504, 1991.

[10] S. Park, J. Deyst, and J. How, "A new nonlinear guidance logic for trajectory tracking," *AIAA Guidance, Navigation and Control Conference and Exhibit*, Jan 2004.

[11] S. Park, J. Deyst, and J. P. How, "Performance and Lyapunov stability of a nonlinear path-following guidance method," *Journal of Guidance, Control and Dynamics*, vol. 30, no. 6, p. 1718, 2007.

[12] R. Curry, M. Lizarraga, G. Elkaim, and B. Mairs, "$\mathcal{L}_2^+$, an improved line of sight guidance law for UAVs," in *American Control Conference, ACC*, Washington, D.C., June 2013.

[13] M. Lizarraga, "Design, implementation and flight verification of a versatile and rapidly reconfigurable uav gnc research platform," Ph.D. dissertation, Department of Computer Engineering, University of California Santa Cruz, Santa Cruz, CA, December 2009.

[14] M. Lizarraga, G. H. Elkaim, G. Horn, R. Curry, V. Dobrokhodov, and I. Kaminer, "Low cost rapidly reconfigurable uav autopilot for research and development of guidance, navigation and control algorithms," in

International Conference on Mechatronic and Embedded Systems and Applications, San Diego, CA, August 2009.

[15] M. Lizarraga, R. Curry, G. Elkaim, and B. Mairs, "SLUGS UAV: A Flexible and Versatile Hardware/Software Platform for Guidance Navigation and Control Research," in *American Control Conference, ACC*, Washington, D.C., June 2013.